

# ScribbleVS: Scribble-Supervised Medical Image Segmentation via Dynamic Competitive Pseudo Label Selection

Tao Wang<sup>a</sup>, Xinlin Zhang<sup>a</sup>, Yuanbin Chen<sup>a</sup>, Yuanbo Zhou<sup>a</sup>, Longxuan Zhao<sup>a</sup>, Tao Tan<sup>b</sup> and Tong Tong<sup>a,\*</sup>

<sup>a</sup>College of physics and information engineering, Fuzhou University, Xueyuan Road No.2, Fuzhou, 350108, Fujian, China

<sup>b</sup>Faculty of Applied Science, Macao Polytechnic University, Macao, 999078, Macao, China

## ARTICLE INFO

### Keywords:

Medical image segmentation  
Scribble annotation  
Pseudo labels  
Weakly-supervised learning

## ABSTRACT

In clinical medicine, precise image segmentation can provide substantial support to clinicians. However, achieving such precision often requires a large amount of finely annotated data, which can be costly. Scribble annotation presents a more efficient alternative, boosting labeling efficiency. However, utilizing such minimal supervision for medical image segmentation training, especially with scribble annotations, poses significant challenges. To address these challenges, we introduce ScribbleVS, a novel framework that leverages scribble annotations. We introduce a Regional Pseudo Labels Diffusion Module to expand the scope of supervision and reduce the impact of noise present in pseudo labels. Additionally, we propose a Dynamic Competitive Selection module for enhanced refinement in selecting pseudo labels. Experiments conducted on the ACDC and MSCMRseg datasets have demonstrated promising results, achieving performance levels that even exceed those of fully supervised methodologies. The codes of this study are available at <https://github.com/ortonwang/ScribbleVS>.

## 1. Introduction

In recent years, deep neural networks have demonstrated their potential across diverse visual tasks [14], from object recognition to scene comprehension. They have also achieved notable successes in medical image segmentation [35][33]. Precise image segmentation within clinical medical practice offers clinicians crucial auxiliary data, facilitating swift and precise diagnostic decisions [1].

However, the success of these methods relies on comprehensive manual annotations, necessitating detailed and intensive labor. In medical imaging, annotating a single image can demand hours from an experienced physician, necessitating considerable expertise and resources [49] [28]. To address these issues, some approaches have integrated unlabeled data into model training, utilizing semi-supervised learning (SSL) [45][38][22][47]. Nonetheless, SSL still requires a subset of precisely annotated images, leading to substantial annotation efforts. To improve annotation efficiency, researchers have started exploring segmentation networks based on weak annotations [29], such as scribbles [17], bounding boxes [25], points [2], and image-level labels [26]. Several studies have investigated image-level labels as a basis for segmentation [6][37][36][41], yet these methods often rely on large-scale training datasets and may exhibit poor performance when applied to small medical image datasets. In contrast, scribbles are suitable for annotating nested structures and are easily to obtain in practice, offering significantly higher annotation efficiency compared to dense manual annotation (as shown in the example in Figure 1). Some work has already demonstrated their potential in semantic and medical image segmentation [7][11]. Therefore, we propose to investigate this specific form of weakly

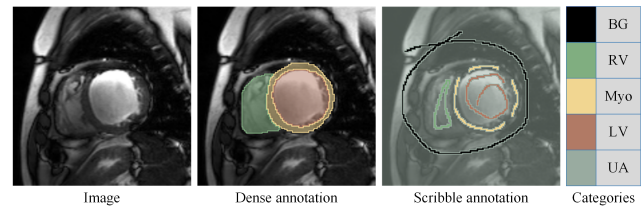


**Figure 1:** Examples of pixel level annotation and scribble annotations. BG, RV, Myo, LV, and UA represent the background, right ventricle, myocardium, left ventricle, and unannotated pixels respectively.

supervised segmentation, which solely relies on scribble annotations for model training, making it more suitable for costly annotation of medical images.

Currently, Several studies have explored and utilized scribble annotation techniques in diverse contexts. Lin *et al.* [18] proposed a graph-based method to propagates information from scribbles to unannotated pixels and train the models jointly. Subsequently, Tang *et al.* [31] introduced Conditional Random Field (CRF) regularization loss into the training of segmentation networks. In the domain of medical imaging, Can *et al.* [4] proposed an iterative framework for model training with scribble annotations. Kim *et al.* [8] introduced a regularization function based on level sets[24] to train deep networks with weak annotations. Lee *et al.* [15] combined pseudo labeling and label filtering to generate reliable labels for network training with scribble annotations. Liu *et al.* [20] proposed a unified weakly supervised framework for training networks from scribble annotations, which consists of an uncertainty-aware mean teacher and a transformation-consistency strategy. Valvano *et al.* [34] introduced a scribble-based segmentation model

\*corresponding author, [traveltong@imperial-vision.com](mailto:traveltong@imperial-vision.com)

[ortonwangtao@gmail.com](mailto:ortonwangtao@gmail.com) (T. Wang)

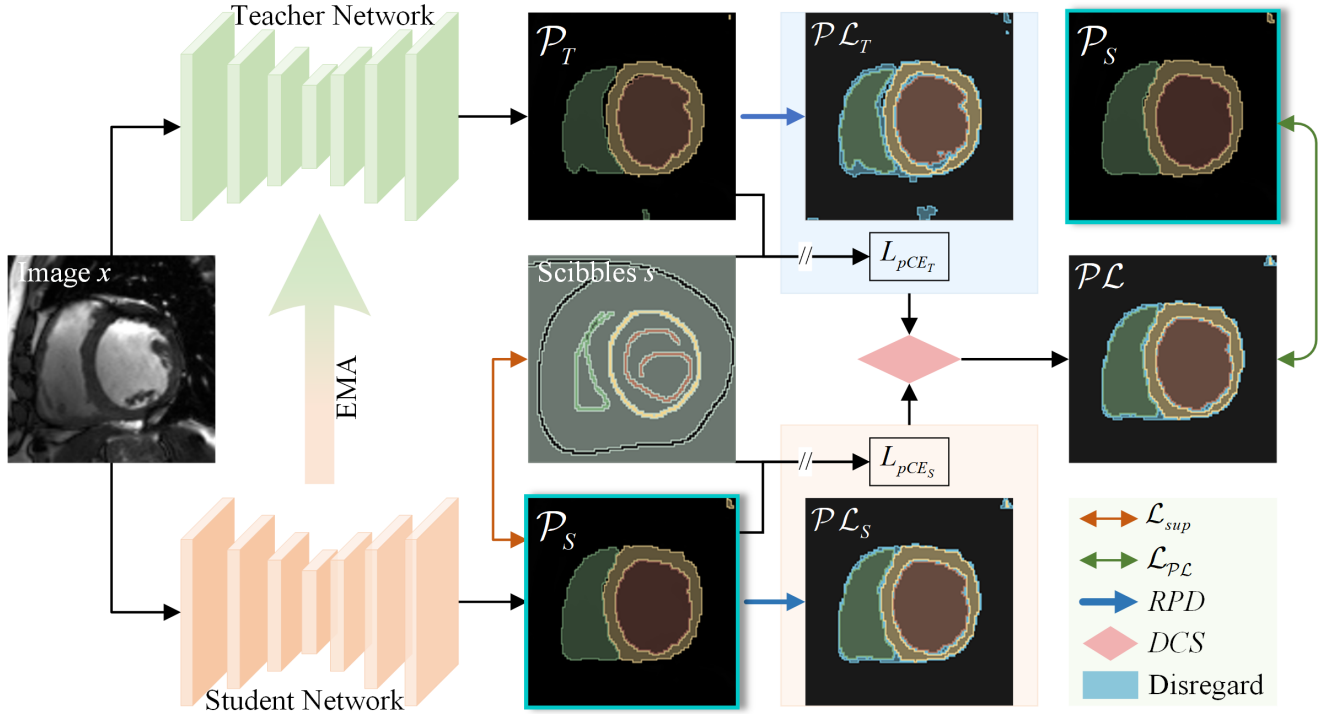


**Figure 2:** The schematic diagram of the proposed ScribbleVS framework, which comprises the *RPD* module and the *DCS* module. The ■ areas in the  $\mathcal{P}\mathcal{L}$  indicate regions to be disregarded when evaluating losses, and the EMA signifies that the teacher network implements parameter updates from the student network through the exponential moving average.

using multi-scale Generative Adversarial Network (GAN) and attention gates mechanism, introducing a novel unpaired segmentation mask strategy that requires additional annotation masks for training. Simultaneously, Luo *et al.* [23] developed a dual-branch framework, employing dynamically mixed pseudo label supervision (DMPLS) for scribble-annotated medical image segmentation. Further, Cyclemix [43] was employed to generate blended images, enhancing the training goal with consistency losses to address inconsistent segmentations. Li *et al.* presented ScribbleVC [16], integrating scribble-based methods with segmentation networks and class embedding modules for enhanced segmentation masks.

Although scribble annotations can reduce the necessity for extensive, expert-driven annotation efforts, their constrained supervisory signals could affect model precision. Furthermore, medical images often exhibit various quality defects that may adversely affect model performance. Yet, the critical accuracy requirements of medical imaging tasks underscore the need for further enhancement of algorithm accuracy. To this end, we introduce ScribbleVS, a novel framework tailored for medical image segmentation with scribble annotations. Overall, the main contributions of this paper are as follows:

- We introduce ScribbleVS, a novel framework based on a mean teacher network for scribble-annotated training.

- We launch a Regional Pseudo labels Diffusion Module to expand supervisory scope, enabling the use of pseudo labels while minimizing noise.
- We propose a Dynamic Competition Selection Module to boost the model's robustness by selectively using appropriate pseudo labels for training.
- Experimental results on ACDC and MSCMRseg dataset demonstrate promising improvements over previous state-of-the-art methods, achieving segmentation precision surpassing that of fully-supervised models.

## 2. Methods

Fig. 2 illustrates ScribbleVS, which is built upon a mean-teacher network, this framework incorporates the Regional Pseudo labels Diffusion (*RPD*) and Dynamic Competition Selection (*DCS*) modules. During the training process, the teacher network does not have gradients, instead, its parameters are updated from the student network through the exponential moving average. The initial learning is conducted using scribble annotations through  $\mathcal{L}_{sup}$ . Following this, the *RPD* Module generates pseudo labels to broaden the scope of supervision. The *DCS* module then dynamically selects pseudo labels throughout the training process. Detailed insights into each module are provided in the subsequent subsections.

## 2.1. Scribble Supervision Module

For scribble annotation learning, we utilize the images along with their corresponding scribble annotations. These annotations exclusively identify pixels with specific classes or unknown labels. Consequently, the model is trained by minimizing the partial cross-entropy loss ( $\mathcal{L}_{pCE}$ ), denoted as  $\mathcal{L}_{sup}$  in Fig. 2. The specific formula is defined as follows:

$$\mathcal{L}_{pCE}(p, s) = - \sum_{i \in \Omega_l} \sum_{k \in K} s[i, k] \cdot \log p[i, k] \quad (1)$$

Where  $K$  represents the index set of labels within the image, and  $\Omega_l$  denotes the set of labeled pixels in the scribble  $s$ . Here,  $s[i, k]$  and  $p[i, k]$  represent the probability that the  $i$ -th pixel belongs to the  $k$ -th category in the scribble and the prediction, respectively.

## 2.2. Regional Pseudo Labels Diffusion Module

Contrary to approaches that generate pseudo labels for all regions[23], we introduce a Regional Pseudo Labels Diffusion ( $RPD$ ) module. We commence by normalizing the prediction, which is computed by:

$$Pre = \text{Softmax}(f_\theta(x)) \quad (2)$$

where  $\theta$  represents the parameters of the network. Following this, departing from conventional sharpening approaches to generate pseudo-label, we introduce a threshold  $\tau$  to identify regions exceeding or below this confidence level, represented by  $\Omega$  and  $\Theta$ . The specific formula is detailed below:

$$\Omega, \Theta = Pre > \tau, Pre \leq \tau \quad (3)$$

These steps facilitate the extraction of highly confident regions. Subsequently, by merging  $Pre$  and  $\Omega$ , we derive the corresponding pseudo labels. The formula for this process is articulated as follows:

$$A_{pre} = \text{Argmax}(Pre) \quad (4)$$

$$\mathcal{P}\mathcal{L} = \text{Merge}(A_{pre} \wedge \Omega, \phi(\Theta)) \quad (5)$$

where  $\phi$  means encoding the regions into disregarded and the  $\mathcal{P}\mathcal{L}$  indicates the pseudo labels generated via the  $RPD$ . This module strives to exclude less reliable areas to minimizing the introduction of noise into pseudo labels. Through the  $RPD$  module, the scribble annotations are extended to the unlabeled pixels, thus broadening the scope of supervision from mere scribbles to the entire image. The evolution of generated pseudo-labels is depicted in Fig. 4.

## 2.3. Dynamic Competition Selection Module

Algorithm 1 provides a comprehensive delineation of our proposed Dynamic Competitive Selection ( $DCS$ ) module. Leveraging the predictions  $\mathcal{P}_S$  and  $\mathcal{P}_T$  from the student and teacher networks, respectively, we employ the  $\mathcal{L}_{pCE}$  to quantify the discrepancies of  $\mathcal{P}_S$  and  $\mathcal{P}_T$  against the scribble

---

### Algorithm 1 Dynamic Competition Selection Module

---

**Require:**

 The image  $x$  and corresponding scribble annotation  $s$ 

 The Teacher Network  $f_T(\cdot)$  and the Student Network:  $f_S(\cdot)$ 

```

1:  $\mathcal{L}_{pCE_S} \leftarrow 0;$             $\mathcal{L}_{pCE_T} \leftarrow 0$ 
2:  $\mathcal{P}_S \leftarrow f_S(x),$         $\mathcal{P}_T \leftarrow f_T(x)$ 
3:  $L_{pCE_S} \leftarrow \mathcal{L}_{pCE}(\mathcal{P}_S, s),$     $L_{pCE_T} \leftarrow \mathcal{L}_{pCE}(\mathcal{P}_T, s)$ 
4: if  $L_{pCE_S} \leq L_{pCE_T}$  then
5:    $\mathcal{P}\mathcal{L} \leftarrow \mathcal{P}\mathcal{L}_S \leftarrow RPD(\mathcal{P}_S)$ 
6: else
7:    $\mathcal{P}\mathcal{L} \leftarrow \mathcal{P}\mathcal{L}_T \leftarrow RPD(\mathcal{P}_T)$ 
8: end if
9: return  $\mathcal{P}\mathcal{L}$ 

```

---

annotations  $s$ , resulting in  $L_{pCE_S}$  and  $L_{pCE_T}$ . A lower loss value signifies a more precise congruence within the scribble annotations. We posit that network demonstrating superior performance tend to exhibit enhanced performance across the entire image. Therefore, we use this insight to convert the respective predictions into pseudo labels via the  $RPD$ . Following this step, we introduce  $\mathcal{L}_{p\mathcal{L}}$  to evaluate the loss between  $\mathcal{P}_S$  and  $\mathcal{P}\mathcal{L}$ . The formulations for  $\mathcal{L}_{p\mathcal{L}}$  are provided as follows:

$$\mathcal{L}_{p\mathcal{L}CE}(p, \mathcal{P}\mathcal{L}) = - \sum_{i \in \Omega} \sum_{k \in K} \mathcal{P}\mathcal{L}[i, k] \cdot \log p[i, k] \quad (6)$$

$$\mathcal{L}_{p\mathcal{L}Dc}(p, \mathcal{P}\mathcal{L}) = 1 - \frac{2 \cdot \sum_{i \in \Omega} \sum_{k \in K} p[i, k] \cdot \mathcal{P}\mathcal{L}[i, k]}{\sum_{i \in \Omega} \sum_{k \in K} p[i, k]^2 + \sum_{i \in \Omega} \sum_{k \in K} \mathcal{P}\mathcal{L}[i, k]^2} \quad (7)$$

$$\mathcal{L}_{p\mathcal{L}} = \frac{1}{2} (\mathcal{L}_{p\mathcal{L}CE}(\mathcal{P}_S, \mathcal{P}\mathcal{L}) + \mathcal{L}_{p\mathcal{L}Dc}(\mathcal{P}_S, \mathcal{P}\mathcal{L})) \quad (8)$$

where  $K$  represents the set of label indices within the  $\mathcal{P}\mathcal{L}$ , and the  $\Omega$  denotes the regions considered in the  $\mathcal{P}\mathcal{L}$ .  $\mathcal{P}\mathcal{L}[i, k]$  and  $p[i, k]$  indicate the probability that the  $i$ -th pixel is classified into the  $k$ -th category in the  $\mathcal{P}\mathcal{L}$  and the prediction, respectively.

## 2.4. Total Loss Function

The ScribbleVS framework is designed to facilitate learning from scribble annotation and the generated  $\mathcal{P}\mathcal{L}$ , by optimizing comprehensive objective function:

$$\mathcal{L}_{total} = \mathcal{L}_{sup} + \lambda \cdot \mathcal{L}_{p\mathcal{L}} \quad (9)$$

the  $\mathcal{L}_{p\mathcal{L}}$  is already illustrated in equations 8. We employ  $\lambda(t)$ , a widely used time-dependent Gaussian warming-up function [12], to balance the contributions between  $\mathcal{L}_{sup}$  and  $\mathcal{L}_{p\mathcal{L}}$  across different phases of the training process. The specific formula is defined as follows:

$$\lambda(t) = \begin{cases} e^{(-5(1-\frac{t}{t_{warm}})^2)} & t < t_{warm} \\ 1 & t \geq t_{warm} \end{cases} \quad (10)$$

Where  $t$  represents the current training step, and  $t_{warm}$  denotes the maximum warming-up step.

**Table 1**

The performance (Dice Scores) on ACDC and MSCMRseg dataset of ScribbleVS compared with different SOTA method. Bold denotes the best performance, underline denotes the second-best performance.

Methods	Data	ACDC				MSCMRseg			
		LV	MYO	RV	Avg	LV	MYO	RV	Avg
U-Net <sub>pCE</sub> [30]	scribbles	.842	.764	.693	.766	.749	.637	.681	.689
U-Net <sub>pCE</sub> <sup>++</sup> [47]	scribbles	.846	.787	.652	.761	.497	.506	.472	.492
MixUp [42]	scribbles	.803	.753	.767	.774	.610	.463	.378	.484
Cutout [5]	scribbles	.832	.754	.812	.800	.459	.641	.697	.599
CutMix [40]	scribbles	.641	.734	.740	.705	.578	.622	.761	.654
Puzzle Mix [10]	scribbles	.663	.650	.559	.624	.061	.634	.028	.241
Co-mixup [9]	scribbles	.622	.621	.702	.648	.356	.343	.053	.251
CycleMix [43]	scribbles	.883	.798	.863	.848	.870	.739	.791	.800
DMPLS [23]	scribbles	.875	<b>.903</b>	.852	.870	.881	.644	<u>.863</u>	.796
ScribbleVC [16]	scribbles	<u>.914</u>	.866	<u>.870</u>	<u>.884</u>	<u>.921</u>	<u>.830</u>	<u>.852</u>	<u>.868</u>
ScribbleVS(Ours)	scribbles	<b>.929</b>	<u>.894</u>	<b>.895</b>	<b>.906</b>	<b>.936</b>	<b>.858</b>	<b>.866</b>	<b>.887</b>

### 3. Experiments and Results

#### 3.1. Dataset

In this paper, we evaluated the proposed ScribbleVS framework and compared it with state-of-the-art (SOTA) method using two publicly available datasets: the ACDC dataset and the MSCMRseg dataset. Additionally, we conducted extensive parameter studies using the ACDC dataset.

##### 3.1.1. ACDC dataset

The ACDC dataset[3] consists of 2D cine-MRI images collected from 100 patients, acquired using two MRI scanners with different magnetic strengths and resolutions. For each patient, manual annotations of right ventricle (RV), left ventricle (LV) and myocardium (MYO) are provided for both the end-diastolic and end-systolic phase. The manual annotations were provided by [34]. Following them, 70 scans were allocated for training, 15 for validation, and the remaining 15 were reserved for testing purposes. To compare with SOTA methods, which employed unpaired mask learning for shape priors, we further divided the training set into two subsets: 35 training images with scribble labels and 35 mask images with heart segmentation. Notably, these corresponding masks were not utilized during training.

##### 3.1.2. MSCMRseg dataset

The MSCMRseg dataset [50][48] comprises late gadolinium enhancement (LGE) MRI images collected from 45 patients diagnosed with cardiomyopathy. These images pose greater challenges for automatic segmentation when compared to unenhanced cardiac MRI scans. Organizers have made available gold standard segmentations of the LV, MYO, and RV within these images. Furthermore, annotations with scribbles for LV, MYO, and RV were provided by the authors in [43]. Following [39], we allocated 25 scans for training, 5 for validation, and reserved the remaining 15 scans for testing.

#### 3.2. Implementation Details

We employed the U-Net [27] as the fundamental segmentation network for a fair comparison. Our framework was implemented using PyTorch 1.12.0, leveraging an Nvidia RTX 3090 GPU with 24GB of memory. Initially, the intensity of each slice was rescaled to fit within the range of 0-1 for network training. Random rotation and flipping were employed to augment the training set. The augmented images were resized to  $256 \times 256$  as input for the network. For model optimization, we employed SGD with weight decay of  $10^{-4}$  and momentum of 0.9 to minimize the joint loss function  $\mathcal{L}_{total}$ . The poly learning rate strategy was adopted to dynamically adjust the learning rate [21]. The batch size, total iterations,  $\tau$  and  $t_{warm}$  were set to 12, 60k, and 12k, respectively. During testing, predictions were generated slice-by-slice and subsequently assembled into a 3D volume. To maintain fair comparisons, we utilized the output of the student network as the final result during inference without applying any post-processing methods. All experiments were conducted under a consistent experimental setup. The Dice coefficient was used as the evaluation metric to assess performance on both datasets.

#### 3.3. Performance Comparison with Other SOTA Methods

To demonstrate the comprehensive segmentation performance of our method, we compared ScribbleVS with various SOTA methods.

##### 3.3.1. Baselines

Initially, we compared ScribbleVS with the U-Net [27] using the partial cross-entropy loss. Subsequently, we compared our method with various data augmentation strategies: including MixUp [42], Cutout [5], CutMix [40], Puzzle Mix [10], Co-mixup [9], and Cyclemix [43]. Moreover, we included comparisons with the latest methodologies, DMPLS [23] and ScribbleVC [16] for comparison. For a comprehensive evaluation, we referred to the experimental

results reported in [34] on the ACDC dataset, namely U-Net<sub>pCE</sub> [30], U-Net<sub>wpCE</sub> [34], U-Net<sub>CRF</sub> [46].

### 3.3.2. Challenging benchmarks

The above methods did not utilize extra unpaired segmentation masks during training. For a more rigorous benchmark, we compared our method with four approaches that incorporated shape priors using additional unpaired data: Post-DAE [13], U-Net<sub>D</sub> [34], ACCL [44], and MAAG [34]. The segmentation results of these methods were compared on the ACDC dataset as reported in [34]. Additionally, we performed a comparative analysis involving semi-supervised learning approaches. We used 7 labeled subjects and 28 unlabeled subjects for training to mirror the annotation costs associated with scribble annotations. The evaluation encompassed four prevalent semi-supervised segmentation methods: MT [32], UAMT [38], SLC-Net [19], and URPC [22].

### 3.4. Comparison with SOTA Methods

Table 1 illustrates the performance of ScribbleVS on the ACDC and MSCMRseg datasets. Our ScribbleVS model, guided by scribble annotation, demonstrates superior performance compared to various training strategies, model architectures, and data augmentation techniques based on U-Net in terms of scribble supervision. Specifically, ScribbleVS shows a 2.2% (90.6% vs 88.4%) improvement on the ACDC dataset and a 1.9% (88.7% vs 86.8%) improvement on the MSCMRseg dataset compared to the SOTA method ScribbleVC. These results underscore the effectiveness of our approach in medical image segmentation guided by scribble annotations. Conversely, with only scribble annotations available, U-Net<sub>pCE</sub> exhibited weaker performance, achieving Dice scores of 76.6% and 68.9% on the two datasets, respectively. Particularly, significant performance degradation was noted on the MSCMRseg dataset, highlighting the adaptability of our framework in handling datasets with more segmentation complexities. Additionally, compared to DMPLS, our framework exhibited a notable improvement of 3.6% (90.6% vs 87.0%) on the ACDC dataset and a substantial 9.1% (88.7% vs 79.6%) on the MSCMRseg dataset. These results emphasize the effectiveness of the pseudo labeling strategy utilized to enhance segmentation performance.

Figure 3 showcases the visual segmentation result of our method and other SOTA methods on the ACDC and MSCMR datasets. From the figure, it is evident that our approach demonstrates closer proximity to the Ground Truth. This visual representation serves as an intuitive demonstration of the effectiveness of our method.

### 3.5. Comparison with weakly-supervised methods

Table 2 presents the results obtained on the ACDC dataset. The best method, MAAG [34], utilized unpaired masks from 35 additional subjects, achieving a Dice Score of 81.6% with multi-scale GAN assistance. ScribbleVS, without these masks, achieves a Dice score of 90.6% on average, demonstrating promising superiority over MAAG. Particularly for the RV structure with substantial shape

**Table 2**

The performance (Dice Scores) on ACDC dataset of ScribbleVS compared with SOTA weakly-supervised methods. We referred to their segmentation results reported in [34] on ACDC dataset for comparison.

Methods	Data	LV	MYO	RV	Avg
35 scribbles					
U-Net <sub>pCE</sub> [30]	scribbles	.842	.764	.693	.766
U-Net <sub>wpCE</sub> [34]	scribbles	.784	.675	.563	.674
U-Net <sub>CRF</sub> [46]	scribbles	.766	.661	.590	.672
ScribbleVS(Ours)	scribbles	<b>.929</b>	<b>.894</b>	<b>.895</b>	<b>.906</b>
35 scribbles + 35 unpaired mask					
U-Net <sub>D</sub> [34]	scribbles+mask	.404	.597	.753	.585
PostDAE [13]	scribbles+mask	.806	.667	.556	.676
ACCL [44]	scribbles+mask	.878	.797	.735	.803
MAAG [34]	scribbles+mask	<b>.879</b>	<b>.817</b>	<b>.752</b>	<b>.816</b>
7 paired mask and 28 unlabeled					
MT [32]	unlabeled+mask	.866	.788	.706	.787
UAMT [38]	unlabeled+mask	.795	.733	.601	.709
SLC-Net [19]	unlabeled+mask	.889	.834	.754	.826
URPC [22]	unlabeled+mask	.863	.774	.700	.779

variations, ScribbleVS obtained a remarkable improvement of 14.3% over MAAG (89.5% vs. 75.2%). Comparative to other methods, ScribbleVS demonstrates more substantial performance improvements. Our findings suggest that GAN-based methods, even with additional masks, can only capture limited shape priors when trained on a restricted image set. Furthermore, when using SSL with 7 labeled subjects and 28 unlabeled subjects, SLC-Net achieve a Dice score of 82.6%, significantly lower than ScribbleVS. This indicates that, under comparable annotation costs, our method can achieve notably superior performance. Furthermore, the upper section of Table 2 clearly illustrates ScribbleVS consistently outperformed over all other scribble-supervised methods, showing an average performance increase of up to 14.0% compared to U-Net<sub>pCE</sub>, which ranks second.

### 3.6. Evolution of Pseudo Labels by PLGM

Figure 4 illustrates the evolution of pseudo-labels generated through the *RPD* and *argmax* processes during training. As training progresses, the model gradually improves its ability to distinguish targets. Initially, after 100 iterations, the majority of regions generated by *RPD* are marked as disregarded for loss computation, while those produced by *argmax* contain substantial noise. As training continues, the regions labeled as disregarded by *RPD* gradually decrease. Simultaneously, with fewer training iterations, the boundary regions between different segmentation categories exhibit more uncertainty. However, with continued training, the disparity between these segmentation categories gradually diminishes. This demonstrates an enhancement in the model's recognition capability, allowing for a more confident identification of the characteristic boundaries within each segmentation region. Compared to the *argmax* operation, our *RPD* module skips regions with insufficient confidence during training, thereby minimizing the introduction of noise into the pseudo labels and enhancing the model's robustness.

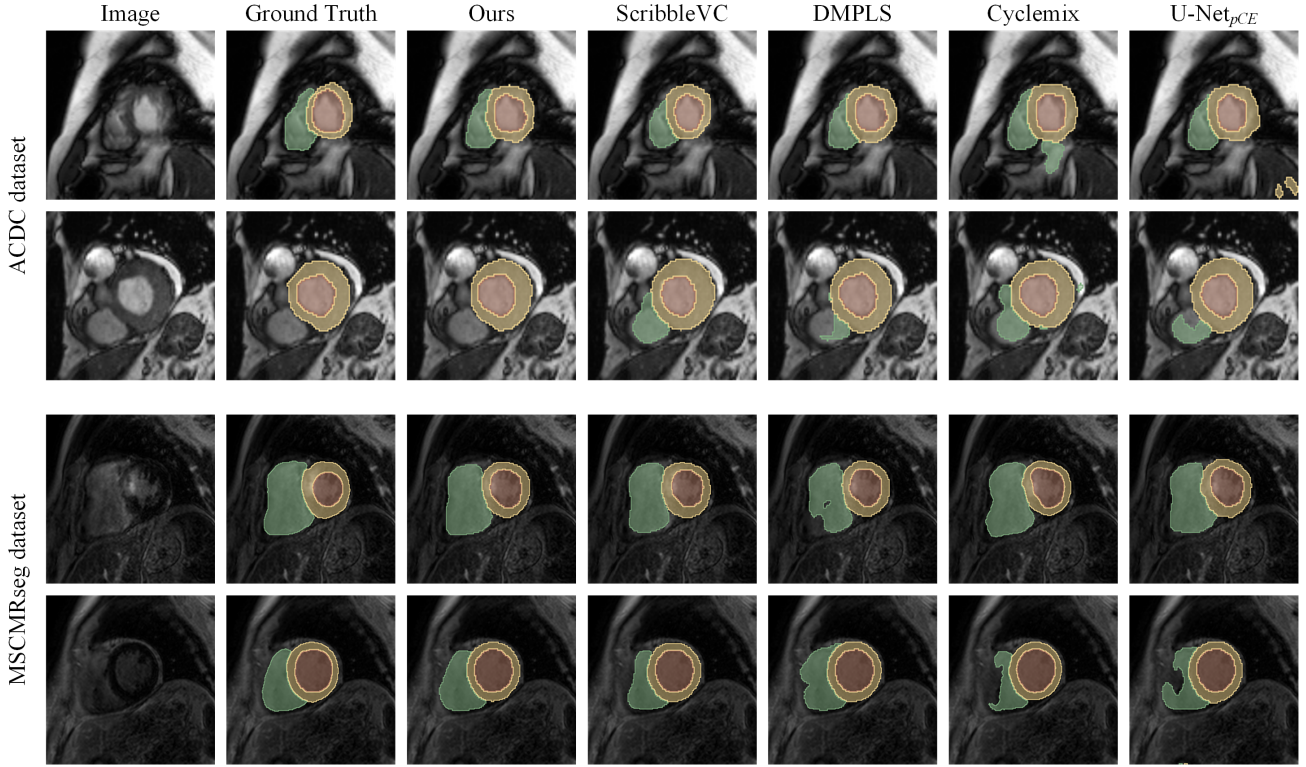


**Figure 3:** Visualization with other methods on the ACDC and MSCMRseg datasets. The models are trained with scribble annotations.

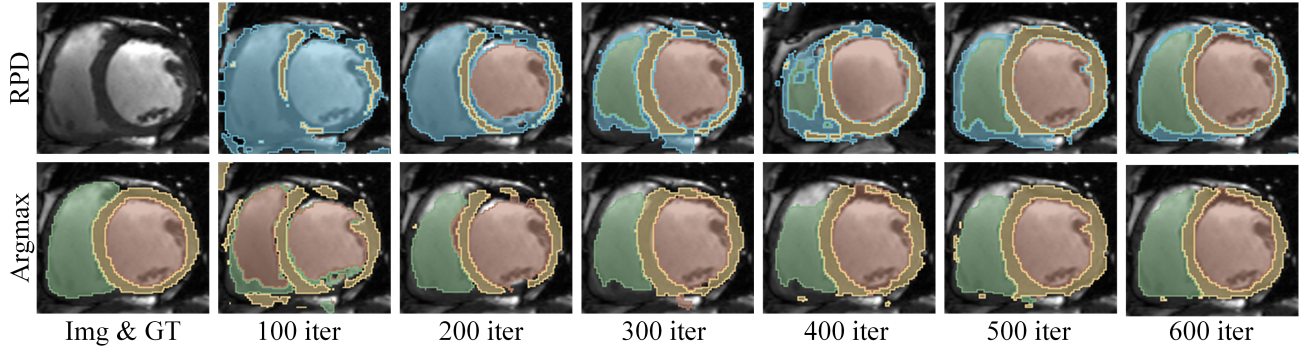


**Figure 4:** Evolution of pseudo labels generated by the *RPD* and the argmax processing. The ■ areas indicate regions that are disregarded when computing losses.

### 3.7. Ablation study

#### 3.7.1. Effect of the combined modules

We conducted an ablation analysis of ScribbleVS, evaluating its components: the *RPD*, direct conversion of teacher network predictions into pseudo-labels via *RPD*, and the incorporation of *DCS*. The summarized results are presented in Table 3. Utilizing solely our *RPD* resulted in a Dice score of 89.5%, underscoring its superiority. When integrated into the mean teacher framework alongside *DCS*, the model exhibited further improvement, achieving a Dice score of 90.6%. This highlights the effectiveness of employing a dynamic competitive approach to select networks, contributing to improving the precision of pseudo labels

**Table 3**

Ablation study about the combination of modules on the ACDC dataset. The Arg represents the pseudo labels generated by the Argmax process directly.

Arg	<i>RPD</i>	<i>DCS</i>	LV	MYO	RV	Avg
✓			0.815	0.804	0.797	0.805
	✓		<b>0.930</b>	0.877	0.877	0.895
✓		✓	0.929	0.881	0.866	0.892
	✓	✓	0.929	<b>0.894</b>	<b>0.895</b>	<b>0.906</b>

and consequently advancing model training and reinforcing robustness.

### 3.7.2. Effect of the hyperparameter $\tau$

To enhance the precision of pseudo labels, this study introduces *RPD* and incorporates a hyperparameter,  $\tau$ . Regions within the pseudo labels are only considered when the confidence exceeds  $\tau$ . Figure 5 displays the experimental results on the ACDC and MSCMRseg datasets for different  $\tau$  values. A smaller  $\tau$  may result in more noise within the pseudo labels, while a larger  $\tau$  could reduce coverage of targeted regions within them, thereby diminishing the supervision effect and impacting the model’s performance.

The experimental results demonstrate that in the ACDC dataset, the model achieved the best Dice score of 90.6 when  $\tau$  was set to 0.5 and 0.55. On the other hand, in the MSCMRseg dataset, the model attained the best performance with a Dice score of 88.7% at  $\tau=0.5$ , slightly outperforming the results at  $\tau=0.55$ . Consequently, we selected  $\tau=0.5$  for subsequent experiments. Notably, in the more challenging segmentation task of the MSCMR dataset, variations in  $\tau$  notably impacted the experimental outcomes, further emphasizing the effectiveness of our *RPD* module in handling complex segmentation tasks.

It’s worth noting that both datasets in this study involve a four-category segmentation task, rather than a binary one. In the four-category task, when  $\tau$  is set to 0.25, our *RPD* operates equivalent to the argmax operation. Moreover, the experimental results clearly indicate the superiority of our approach over the argmax operation.

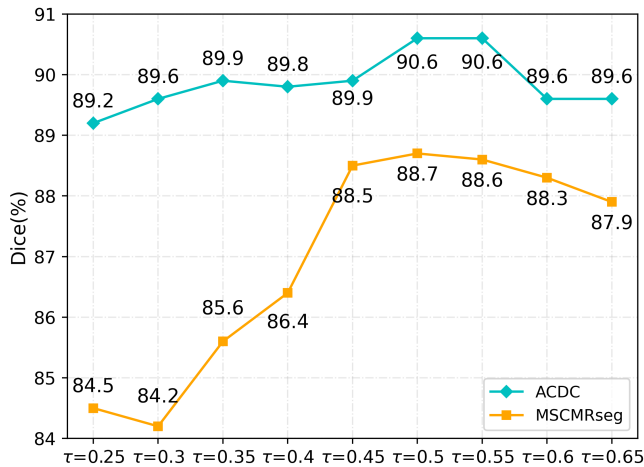


**Figure 5:** Ablation study: the performance of ScribbleVS with different  $\tau$  on the ACDC dataset and MSCMRseg dataset.

### 3.7.3. Data Sensitivity Experiments

The data sensitivity analysis aims to investigate the performance of ScribbleVS across varying quantities of scribble-annotated samples. As depicted in Table 6, ScribbleVS exhibits a consistent enhancement in performance with an increasing number of annotated scribble samples. Notably, it achieves a Dice score of 76.4% using merely 10 annotated training samples. Subsequently, with an increase to 20 annotated samples, our model achieved a Dice score

**Table 4**

Data sensitivity study: the performance of ScribbleVS with the different numbers of scribbles for training.

Method	Scribble Data	LV	MYO	RV	Avg
ScribbleVS	10 scribbles	.840	.710	.744	.764
ScribbleVS	15 scribbles	.848	.837	.642	.776
ScribbleVS	20 scribbles	.926	.874	.852	.884
ScribbleVS	25 scribbles	.926	.888	.885	.900
ScribbleVS	30 scribbles	<b>.935</b>	.891	.883	.903
ScribbleVS	35 scribbles	.929	<b>.894</b>	<b>.895</b>	<b>.906</b>

**Table 5**

Comparisons on fully-supervised and scribble-supervised segmentation.

ACDC dataset					
Method	Annotation	LV	MYO	RV	Avg
U-Net	Dense Annotation	.927	.897	.886	.903
ScribbleVS	Scribble Annotation	.929	.894	.895	.906
ScribbleVS	Dense Annotation	<b>.942</b>	<b>.901</b>	<b>.902</b>	<b>.918</b>
MSCMRseg dataset					
Method	Annotation	LV	MYO	RV	Avg
U-Net	Dense Annotation	.923	.833	.851	.869
ScribbleVS	Scribble Annotation	<b>.936</b>	<b>.858</b>	<b>.866</b>	<b>.887</b>
ScribbleVS	Dense Annotation	.933	.857	.853	.881

of 88.4%. These results emphasize ScribbleVS’s remarkable robustness, even when trained with a limited quantity of annotated scribble data. This resilience underscores its potential utility in resource-constrained environments, where annotated data availability is restricted.

### 3.7.4. Experiments on fully-annotated data

Table 5 provides the Dice scores of fully supervised segmentation on the ACDC and MSCMRseg dataset. Under fully labeled conditions, ScribbleVS showcased its competitiveness by elevating the average Dice score from 90.3% to 91.8% compared to U-Net on the ACDC, and from 86.9% to 88.1% on MSCMRseg. Notably, when leveraging scribble annotations, ScribbleVS achieved an average Dice score of 90.6% and 88.7% on the two dataset, slightly surpassing the Dice score obtained using dense annotations. This highlights ScribbleVS’s remarkable performance in both scribble and fully supervised tasks. Notably, its advantage could be more evident in scribble supervision tasks, aligning with its tailored design for such specific applications.

## 4. Conclusion

In this work, we present ScribbleVS, a novel framework designed for medical image segmentation using scribble-based supervision. To augment supervision efficacy and diminish the impact of noise within pseudo labels, we introduce the Regional Pseudo-label Diffusion (*RPD*) module, which incrementally extends scribble annotations throughout the image. Furthermore, the Dynamic Competitive Selection (*DCS*) module is proposed to dynamically select pseudo labels for training, enhancing the framework’s adaptability. ScribbleVS has been validated as effective, achieving precise pixel-level segmentation outcomes. Comprehensive

assessments on the ACDC dataset highlight the superior performance of our framework over current methodologies. Moving forward, our objective is to expand the application of this framework and conduct rigorous evaluations across a wider array of medical image segmentation challenges.

## 5. Acknowledge

This work was supported by National Natural Science Foundation of China under Grant 62171133.

## References

- [1] Anwar, S.M., Majid, M., Qayyum, A., Awais, M., Alnowami, M., Khan, M.K., 2018. Medical Image Analysis using Convolutional Neural Networks: A Review. *Journal of Medical Systems* 42, 1–13.
- [2] Bearman, Amy and Russakovsky, Olga and Ferrari, Vittorio and Fei-Fei, Li, 2016. What's the Point: Semantic Segmentation with Point Supervision, in: *Computer Vision – ECCV 2016*, pp. 549–565.
- [3] Bernard, O., Lalonde, A., Zotti, C., Cervensky, F., Yang, X., Heng, P.A., Cetin, I., Lekadir, K., Camara, O., Gonzalez Ballester, M.A., Sanroma, G., Napel, S., Petersen, S., Tziritas, G., Grinias, E., Khened, M., Kollerathu, V.A., Krishnamurthi, G., Rohé, M.M., Pennec, X., Sermesant, M., Isensee, F., Jäger, P., Maier-Hein, K.H., Full, P.M., Wolf, I., Engelhardt, S., Baumgartner, C.F., Koch, L.M., Wolterink, J.M., Išgum, I., Jang, Y., Hong, Y., Patravali, J., Jain, S., Humbert, O., Jodoin, P.M., 2018. Deep Learning Techniques for Automatic MRI Cardiac Multi-Structures Segmentation and Diagnosis: Is the Problem Solved? *IEEE Transactions on Medical Imaging* 37, 2514–2525.
- [4] Can, Yigit B., Chaitanya, Krishna, Mustafa, Basil, Koch, Lisa M., Konukoglu, Ender and Baumgartner, Christian F., 2018. Learning to Segment Medical Images with Scribble-Supervision Alone, in: *Deep Learning in Medical Image Analysis and Multimodal Learning for Clinical Decision Support*, pp. 236–244.
- [5] DeVries, T., Taylor, G.W., 2017. Improved regularization of convolutional neural networks with cutout. *arXiv preprint arXiv:1708.04552*.
- [6] Huang, Z., Wang, X., Wang, J., Liu, W., Wang, J., 2018. Weakly-Supervised Semantic Segmentation Network With Deep Seeded Region Growing, in: *Proceedings of the IEEE Conference on Computer Vision and Pattern Recognition (CVPR)*.
- [7] Khoreva, A., Benenson, R., Hosang, J., Hein, M., Schiele, B., 2017. Simple Does It: Weakly Supervised Instance and Semantic Segmentation, in: *Proceedings of the IEEE Conference on Computer Vision and Pattern Recognition (CVPR)*.
- [8] Kim, B., Ye, J.C., 2020. Mumford–Shah Loss Functional for Image Segmentation With Deep Learning. *IEEE Transactions on Image Processing* 29, 1856–1866.
- [9] Kim, J.H., Choo, W., Jeong, H., Song, H.O., 2021. Co-mixup: Saliency guided joint mixup with supermodular diversity. *arXiv preprint arXiv:2102.03065*.
- [10] Kim, J.H., Choo, W., Song, H.O., 2020. Puzzle mix: Exploiting saliency and local statistics for optimal mixup, in: *International Conference on Machine Learning, PMLR*. pp. 5275–5285.
- [11] Koch, L.M., Rajchl, M., Bai, W., Baumgartner, C.F., Tong, T., Passerat-Palmbach, J., Aljabar, P., Rueckert, D., 2018. Multi-Atlas Segmentation Using Partially Annotated Data: Methods and Annotation Strategies. *IEEE Transactions on Pattern Analysis and Machine Intelligence* 40, 1683–1696.
- [12] Laine, S., Aila, T., 2016. Temporal ensembling for semi-supervised learning. *arXiv preprint arXiv:1610.02242*.
- [13] Larrazabal, A.J., Martínez, C., Glocker, B., Ferrante, E., 2020. Post-dae: Anatomically plausible segmentation via post-processing with denoising autoencoders. *IEEE Transactions on Medical Imaging* 39, 3813–3820.
- [14] LeCun, Y., Bengio, Y., Hinton, G., 2015. Deep learning. *Nature* 521, 436–444.
- [15] Lee, Hyeonsoo and Jeong, Won-Ki, 2020. Scribble2Label: Scribble-Supervised Cell Segmentation via Self-generating Pseudo-Labels with Consistency, in: *Medical Image Computing and Computer Assisted Intervention – MICCAI*, pp. 14–23.
- [16] Li, Z., Zheng, Y., Luo, X., Shan, D., Hong, Q., 2023. ScribbleVC: Scribble-Supervised Medical Image Segmentation with Vision-Class Embedding, in: *Proceedings of the 31st ACM International Conference on Multimedia*, p. 3384–3393.
- [17] Lin, D., Dai, J., Jia, J., He, K., Sun, J., 2016a. ScribbleSup: Scribble-Supervised Convolutional Networks for Semantic Segmentation, in: *Proceedings of the IEEE Conference on Computer Vision and Pattern Recognition (CVPR)*.
- [18] Lin, D., Dai, J., Jia, J., He, K., Sun, J., 2016b. ScribbleSup: Scribble-Supervised Convolutional Networks for Semantic Segmentation, in: *Proceedings of the IEEE Conference on Computer Vision and Pattern Recognition (CVPR)*.
- [19] Liu, J., Desrosiers, C., Zhou, Y., 2022a. Semi-supervised medical image segmentation using cross-model pseudo-supervision with shape awareness and local context constraints, in: Wang, L., Dou, Q., Fletcher, P.T., Speidel, S., Li, S. (Eds.), *Medical Image Computing and Computer Assisted Intervention – MICCAI*, pp. 140–150.
- [20] Liu, X., Yuan, Q., Gao, Y., He, K., Wang, S., Tang, X., Tang, J., Shen, D., 2022b. Weakly Supervised Segmentation of COVID19 Infection with Scribble Annotation on CT Images. *Pattern Recognition* 122, 108341.
- [21] Luo, X., Liao, W., Chen, J., Song, T., Chen, Y., Zhang, S., Chen, N., Wang, G., Zhang, S., 2021. Efficient Semi-supervised Gross Target Volume of Nasopharyngeal Carcinoma Segmentation via Uncertainty Rectified Pyramid Consistency, in: *Medical Image Computing and Computer Assisted Intervention–MICCAI*, pp. 318–329.
- [22] Luo, X., Wang, G., Liao, W., Chen, J., Song, T., Chen, Y., Zhang, S., Metaxas, D.N., Zhang, S., 2022. Semi-supervised medical image segmentation via uncertainty rectified pyramid consistency. *Medical Image Analysis* 80, 102517.
- [23] Luo, Xiangde and Hu, Minhao and Liao, Wenjun and Zhai, Shuwei and Song, Tao and Wang, Guotai and Zhang, Shaoting, 2022. Scribble-Supervised Medical Image Segmentation via Dual-Branch Network and Dynamically Mixed Pseudo Labels Supervision, in: *Medical Image Computing and Computer Assisted Intervention – MICCAI*, pp. 528–538.
- [24] Mumford, D.B., Shah, J., 1989. Optimal approximations by piecewise smooth functions and associated variational problems. *Communications on Pure and Applied Mathematics* 42, 577–685.
- [25] Papandreou, G., Chen, L.C., Murphy, K.P., Yuille, A.L., 2015. Weakly- and Semi-Supervised Learning of a Deep Convolutional Network for Semantic Image Segmentation, in: *Proceedings of the IEEE International Conference on Computer Vision (ICCV)*.
- [26] Pathak, D., Shelhamer, E., Long, J., Darrell, T., 2014. Fully Convolutional Multi-Class Multiple Instance Learning. *arXiv preprint arXiv:1412.7144*.
- [27] Ronneberger, O., Fischer, P., Brox, T., 2015. U-Net: Convolutional Networks for Biomedical Image Segmentation, in: *Medical Image Computing and Computer-Assisted Intervention–MICCAI 2015: 18th International Conference, Munich, Germany, October 5-9, 2015, Proceedings, Part III* 18, pp. 234–241.
- [28] Sjöberg, C., Lundmark, M., Granberg, C., Johansson, S., Ahnesjö, A., Montelius, A., 2013. Clinical evaluation of multi-atlas based segmentation of lymph node regions in head and neck and prostate cancer patients. *Radiation Oncology* 8, 1–7.
- [29] Tajbakhsh, N., Jeyaseelan, L., Li, Q., Chiang, J.N., Wu, Z., Ding, X., 2020. Embracing imperfect datasets: A review of deep learning solutions for medical image segmentation. *Medical Image Analysis* 63, 101693.
- [30] Tang, M., Djelouah, A., Perazzi, F., Boykov, Y., Schroers, C., 2018a. Normalized cut loss for weakly-supervised cnn segmentation, in: *Proceedings of the IEEE Conference on Computer Vision and Pattern Recognition (CVPR)*.



- [31] Tang, M., Perazzi, F., Djelouah, A., Ben Ayed, I., Schroers, C., Boykov, Y., 2018b. On Regularized Losses for Weakly-supervised CNN Segmentation, in: Proceedings of the European Conference on Computer Vision (ECCV).
- [32] Tarvainen, A., Valpola, H., 2017. Mean teachers are better role models: Weight-averaged consistency targets improve semi-supervised deep learning results. *Advances in Neural Information Processing Systems* 30.
- [33] Valanarasu, Jeya Maria Jose and Patel, Vishal M., 2022. UN-eXt: MLP-Based Rapid Medical Image Segmentation Network, in: *Medical Image Computing and Computer Assisted Intervention – MICCAI*, pp. 23–33.
- [34] Valvano, G., Leo, A., Tsaftaris, S.A., 2021. Learning to Segment From Scribbles Using Multi-Scale Adversarial Attention Gates. *IEEE Transactions on Medical Imaging* 40, 1990–2001.
- [35] Wang, T., Lan, J., Han, Z., Hu, Z., Huang, Y., Deng, Y., Zhang, H., Wang, J., Chen, M., Jiang, H., et al., . O-Net: A Novel Framework With Deep Fusion of CNN and Transformer for Simultaneous Segmentation and Classification. *Frontiers in Neuroscience* 16, 876065.
- [36] Wang, W., Sun, G., Van Gool, L., 2022. Looking Beyond Single Images for Weakly Supervised Semantic Segmentation Learning. *IEEE Transactions on Pattern Analysis and Machine Intelligence* , 1–1.
- [37] Wang, Y., Zhang, J., Kan, M., Shan, S., Chen, X., 2020. Self-Supervised Equivariant Attention Mechanism for Weakly Supervised Semantic Segmentation, in: *Proceedings of the IEEE/CVF Conference on Computer Vision and Pattern Recognition (CVPR)*.
- [38] Yu, L., Wang, S., Li, X., Fu, C.W., Heng, P.A., 2019. Uncertainty-aware self-ensembling model for semi-supervised 3d left atrium segmentation, in: *Medical Image Computing and Computer Assisted Intervention–MICCAI 2019: 22nd International Conference, Shenzhen, China, October 13–17, 2019, Proceedings, Part II* 22, pp. 605–613.
- [39] Yue, Qian and Luo, Xinzhe and Ye, Qing and Xu, Lingchao and Zhuang, Xiahai, 2019. Cardiac Segmentation from LGE MRI Using Deep Neural Network Incorporating Shape and Spatial Priors, in: *Medical Image Computing and Computer Assisted Intervention – MICCAI*, pp. 559–567.
- [40] Yun, S., Han, D., Oh, S.J., Chun, S., Choe, J., Yoo, Y., 2019. Cutmix: Regularization strategy to train strong classifiers with localizable features, in: *Proceedings of the IEEE/CVF International Conference on Computer Vision (ICCV)*, pp. 6023–6032.
- [41] Zhang, B., Xiao, J., Jiao, J., Wei, Y., Zhao, Y., 2022. Affinity Attention Graph Neural Network for Weakly Supervised Semantic Segmentation. *IEEE Transactions on Pattern Analysis and Machine Intelligence* 44, 8082–8096.
- [42] Zhang, H., Cisse, M., Dauphin, Y.N., Lopez-Paz, D., 2017a. Mixup: Beyond empirical risk minimization. *arXiv preprint arXiv:1710.09412* .
- [43] Zhang, K., Zhuang, X., 2022. CycleMix: A Holistic Strategy for Medical Image Segmentation From Scribble Supervision, in: *Proceedings of the IEEE/CVF Conference on Computer Vision and Pattern Recognition (CVPR)*, pp. 11656–11665.
- [44] Zhang, P., Zhong, Y., Li, X., 2020. Accl: Adversarial constrained-cnn loss for weakly supervised medical image segmentation. *arXiv preprint arXiv:2005.00328* .
- [45] Zhang, Y., Yang, L., Chen, J., Fredericksen, M., Hughes, D.P., Chen, D.Z., 2017b. Deep adversarial networks for biomedical image segmentation utilizing unannotated images, in: *Medical Image Computing and Computer Assisted Intervention- MICCAI*, pp. 408–416.
- [46] Zheng, S., Jayasumana, S., Romera-Paredes, B., Vineet, V., Su, Z., Du, D., Huang, C., Torr, P.H.S., 2015. Conditional random fields as recurrent neural networks, in: *Proceedings of the IEEE International Conference on Computer Vision (ICCV)*.
- [47] Zhou, Z., Rahman Siddiquee, M.M., Tajbakhsh, N., Liang, J., 2018. UNet++: A Nested U-Net Architecture for Medical Image Segmentation, in: *Deep Learning in Medical Image Analysis and Multimodal Learning for Clinical Decision Support*, pp. 3–11.
- [48] Zhuang, X., 2019. Multivariate Mixture Model for Myocardial Segmentation Combining Multi-Source Images. *IEEE Transactions on Pattern Analysis and Machine Intelligence* 41, 2933–2946.
- [49] Zhuang, X., Shen, J., 2016. Multi-scale patch and multi-modality atlases for whole heart segmentation of MRI. *Medical Image Analysis* 31, 77–87.
- [50] Zhuang, Xiahai, 2016. Multivariate Mixture Model for Cardiac Segmentation from Multi-Sequence MRI, in: *Medical Image Computing and Computer-Assisted Intervention – MICCAI*, pp. 581–588.